

Research Article

Aqueous Extract of *Sparganii Rhizoma* and *Curcumae Rhizoma* Induces Apoptosis and Inhibits Migration in Human Oral Squamous Cell Carcinoma

Kai-Wei Chang,^{1,2} Chia-Yu Wu,^{3,4} Ting-Yi Renn,⁵ Tsung-Ming Chang^{1,6},
Augusta I-Chin Wei,⁷ Yen-Ying Kung^{1,2,8} and Ju-Fang Liu^{7,9,10}

¹Institute of Traditional Medicine, National Yang Ming Chiao Tung University, Taipei, Taiwan

²Center for Traditional Medicine, Taipei Veterans General Hospital, Taipei, Taiwan

³School of Dental Technology, College of Oral Medicine, Taipei Medical University, Taipei, Taiwan

⁴Division of Oral and Maxillofacial Surgery, Department of Dentistry, Taipei Medical University Hospital, Taipei, Taiwan

⁵Department of Oral and Maxillofacial Pathobiology, Graduate School of Biomedical and Health Sciences, Hiroshima University, Hiroshima, Japan

⁶Institute of Physiology, School of Medicine, National Yang Ming Chiao Tung University, Taipei, Taiwan

⁷Translational Medicine Center, Shin-Kong Wu Ho-Su Memorial Hospital, Taipei, Taiwan

⁸Faculty of Medicine, School of Medicine, National Yang Ming Chiao Tung University, Taipei, Taiwan

⁹School of Oral Hygiene, College of Oral Medicine, Taipei Medical University, Taipei, Taiwan

¹⁰Department of Medical Research, China Medical University Hospital, China Medical University, Taichung, Taiwan

Correspondence should be addressed to Yen-Ying Kung; yykung@vghtpe.gov.tw and Ju-Fang Liu; jufangliu@tmu.edu.tw

Received 19 November 2022; Revised 3 March 2023; Accepted 4 March 2023; Published 25 May 2023

Academic Editor: Swapan Ray

Copyright © 2023 Kai-Wei Chang et al. This is an open access article distributed under the Creative Commons Attribution License, which permits unrestricted use, distribution, and reproduction in any medium, provided the original work is properly cited.

Sparganii Rhizoma and *Curcumae Rhizoma* (SRCR) are natural herbs used in traditional Chinese medicine to treat tumors and activate blood circulation. Previous studies have shown that SRCR possesses notable antitumor activity; however, the mechanism underlying anticancer activity in human oral squamous cell carcinoma (OSCC) has yet to be fully elucidated. The risk factors of OSCC include smoking, alcohol consumption, poor oral hygiene, and human papillomavirus infection. OSCC is highly metastatic and responds poorly to chemotherapy; thus, alternative treatment options are imperative. In this study, we found that SRCR induced death in OSCC cells but not in normal cells (HGF-1 cells). SRCR has also shown to induce the production of reactive oxygen species in OSCC cells, sequentially promoting calcium release and stress in the endoplasmic reticulum, which resulted in mitochondrial dysfunction and subsequent apoptosis. Furthermore, SRCR has shown to inhibit the migration of OSCC cells by reducing matrix metalloproteinase-12 and -13. Our findings demonstrate that SRCR exerts anticancer activities in OSCC by inducing cell apoptosis and suppressing cell migration.

1. Introduction

Oral cancer is the fifth most common cancer cause of mortality in Taiwan and the eighth most common cancer worldwide [1], characterized by a high rate of recurrence and lymph node metastasis [2]. The progression of oral squamous cell carcinoma (OSCC) is partially accelerated by chronic epithelial irritation, which is commonly associated

with tobacco use, alcohol consumption, environmental pollutants, and viral infection [3]. Despite advancements in diagnostic and therapeutic modalities [4], the prognosis for OSCC is generally poor, with an overall 5-year survival rate of less than 50% [5]. OSCC treatments include surgical interventions, chemotherapy, and radiation; however, the high incidence of metastasis makes it exceedingly difficult to eradicate lesions via surgery and/or chemotherapy [6].

Sparganii Rhizoma and *Curcumae Rhizoma* (SRCR) form a herb pair used by practitioners of traditional Chinese medicine (TCM) to activate blood circulation [7]. Previous studies have demonstrated that SRCR also possesses anti-tumor activity far exceeding that of SR or CR alone [8, 9]. SRCR has been shown not only to have potent anti-tumor effects in a human breast cancer cell line (MCF-7), liver cancer cell line (HepG2), and cervix cancer cell line (HeLa) [10], but also to induce apoptotic cell death of lung cancer cell line (NCI-H1975) via the caspase-dependent apoptosis signaling pathway [11]. In addition, SRCR significantly reduces epithelial-mesenchymal transition and Smad3 phosphorylation, leading to the inhibition of cell migration and invasion in triple-negative breast cancer cells [12]. To date, few studies have examined the effect of SRCR on cell apoptosis and migration or its molecular mechanisms in OSCC. In this study, we found that the anti-tumor effects of SRCR involve ROS production, endoplasmic reticulum (ER) stress, and mitochondrial dysfunction, resulting in caspase activation and subsequent cell apoptosis. We also determined that SRCR inhibits the migratory ability of OSCC by reducing matrix metalloproteinases (MMPs). Our findings demonstrate the cell apoptosis and antimetastasis mechanisms of SRCR for the clinical treatment of metastatic human OSCC.

2. Materials and Methods

2.1. Plant Material. *Sparganii Rhizoma* (SR) and *Curcumae Rhizoma* (CR) were obtained from Kaiser Pharmaceutical Co., Ltd. Taiwan.

2.2. Preparation of the SRCR. SR and CR herb samples were shattered to form a powder (1 : 1 w/w; 50 g each). A 100 g sample of the powder was mixed with 500 mL of water at room temperature, allowed to stand for 2 h, and then heated to 100°C and allowed to stand for further 2 h. The mixture was then filtered, concentrated, and lyophilized. The average yield of SRCR was 10.5%. A 50 g sample of SR or CR was prepared using the same method, with the average yield of SR and CR, respectively, being 3.2% and 5.4%.

2.3. Chemicals and Reagents. Fluo-4 acetoxymethyl ester (Fluo-4 AM), 2',7'-dichlorodihydrofluorescein diacetate (H₂DCFDA), MitoProbe™ JC-1 Assay Kit, L-glutamine, DMEM/F-12 medium, DMEM high-glucose medium, streptomycin, penicillin, and trypsin-EDTA were obtained from Thermo Fisher Scientific Inc. (Waltham, MA, USA). z-DEVD-FMK, z-LEHD-FMK, caspase-3, and caspase-9 colorimetric assay kits were obtained from Merck Millipore (Billerica, MA, USA). Primary antibodies were obtained from Cell Signaling Technology (Danvers, MA, USA), Santa Cruz Biotechnology (Dallas, TX, USA), or Genetex (Hsinchu, Taiwan). All other chemicals and reagents were obtained from Sigma-Aldrich (St. Louis, MO, USA).

2.4. Cell Culture. The human oral squamous cell carcinoma (OSCC) cell line SCC4 was acquired from the Bioresource Collection and Research Center (BCRC, Hsinchu, Taiwan). Cells were maintained in complete DMEM/F-12 medium with 2 mM L-glutamine, 10% fetal bovine serum (FBS), 1% nonessential amino acids, 400 ng/mL hydrocortisone, 100 U/mL penicillin, and 100 U/mL streptomycin (Gibco, Waltham, MA, USA).

The human OSCC cell line HSC3 was acquired from Merck (Merck KGaA, Darmstadt, Germany). Human normal gingival fibroblasts (HGF-1) were obtained from the American Type Culture Collection. Both these cell lines were maintained in a complete DMEM high-glucose medium with 10% heat-inactivated FBS, 100 U/mL penicillin, and 100 U/mL streptomycin (Gibco, Waltham, MA, USA).

All cell lines were maintained at 37°C in a humidified atmosphere containing 5% CO₂. Fresh media were replenished at intervals of 48 h.

2.5. Cell Proliferation Assay. A cell counting kit-8 (CCK-8; Sigma-Aldrich, St. Louis, MO, USA) was used to characterize the cytotoxic activity of SRCR. In brief, HGF-1, HSC3, and SCC4 cells (6 × 10³ cells) were seeded in triplicate in a 96-well plate. Following incubating with SR, CR, or SRCR for 48 h, 10 μL of CCK-8 solution was added to each well and incubated for 3–6 h. Cell numbers were measured using a microplate reader at absorption of 450 nm (Bio-Tek, Winooski, VT, USA).

2.6. DAPI Staining. After SRCR treatment for 48 h, SCC4 and HSC3 cells were fixed in a 3.7% formaldehyde solution and permeabilized with 0.05% Triton X-100. The cells were then stained with 4'-6-diamidino-2-phenylindole (DAPI, 1 μg/mL). Images of SCC4 and HSC3 cells were captured using a fluorescence microscope under 200x magnification (Nikon Eclipse Ti and NIS-Elements AR microscope software version 5.02.01).

2.7. Western Blot Analysis. Following treatment with SRCR at various concentrations (0, 30, 60, 120, 240, or 480 μg/mL), total cell lysates of SCC4 and HSC3 cells were obtained, resolved using 8–15% SDS-PAGE, and then transferred to 0.45 μm polyvinylidene membranes (PVDF). The membranes were blocked with 4% bovine serum albumin (Cat. No. A9647; Sigma-Aldrich; Merck KGaA) and then incubated with primary antibodies (1 : 1,000) against Bcl-2 (GTX100064), Bcl-xl (GTX105661), Bax (GTX100063), Bak (GTX109683), calpain I (GTX102340), calpain II (GTX102499), caspase-3 (19677-1-AP), caspase-9 (10380-1-AP), GRP78 (GTX113340), GRP94 (GTX103203), or β-actin (SI-A5441; 1 : 10,000) at 4°C overnight. After three washes of TBST, the membranes were probed using mouse or rabbit secondary antibodies conjugated to peroxidase (1 : 10,000) at room temperature for 1 h. Protein blots were visualized using an ECL substrate (EMD Millipore) and a UVP bio-imaging system (Upland, CA, USA). Each experiment was repeated at least three times.

2.8. Annexin V-FITC and Propidium Iodide (PI) Staining. To evaluate cell death, SCC4 and HSC3 cells (1×10^6 cells) were incubated with different SRCR conditions for 48 h. Cells were then collected and resuspended in Annexin V/PI detection solution (Proteintech, Cat. No. PF00005) as previously described [13]. Death of SCC4 and HSC3 cells was immediately determined using a BD Accuri C5 flow cytometer and BD Accuri C6 software (version 1.0.264.21 BD Biosciences).

2.9. Cell Cycle Analysis. To evaluate the effects of SRCR on cell cycle, SCC4 and HSC3 cells (1×10^6 cells) were incubated with different SRCR conditions for 48 h. The cells were then fixed with 70% ethanol and stained with a propidium iodide (PI) solution (100 $\mu\text{g}/\text{mL}$ DNase-free RNase A, 0.1% Triton-X 100, and 10 $\mu\text{g}/\text{mL}$ PI in PBS). The cell cycle of SCC4 and HSC3 cells was immediately characterized using CytoFLEX (Beckman Coulter, Milan, Italy).

2.10. Ca^{2+} Concentration, Intracellular ROS Production, and Mitochondrial Membrane Potential (MMP). SCC4 and HSC3 cells (1×10^6 cells) were incubated with SRCR at various time points and then stained with the following: Fluo-4 AM (3 μM) for the detection of Ca^{2+} concentration, H_2DCFDA (5 μM) for the measurement of ROS production, and JC-1 (2 μM) for the evaluation of MMP. SCC4 and HSC3 cells were inspected using a BD Accuri C5 flow cytometer in conjunction with BD Accuri C6 software (version 1.0.264.21 BD Biosciences). Images of SCC4 and HSC3 cells were captured using a red/green fluorescence microscope under 200x magnification (Nikon ECLIPSE Ti and NIS-Elements AR microscope software version 5.02.01).

2.11. Caspase Activation Assay. SCC4 and HSC3 cell lysates were incubated with caspase-9 substrate (Ac-LEHD-pNA; Cat No. ATP173) or caspase-3 substrate (Ac-DEVD-pNA; Cat No. APT165; EMD Millipore Corp, Burlington, MA, USA) in accordance with the manufacturer's instructions. Caspase activity was measured at 405 nm using a microplate reader (Bio-Tek Instruments, Winooski, VT, USA). Results were calculated by determining the percent change in activity compared to an untreated control.

2.12. Wound Healing and Cell Movement Assay. Cell movement was characterized by seeding SCC4 and HSC3 cells (3×10^4 cells) in a silicone insert (IB-80209; ibidi GmbH, Gräfelfing, Germany). Following cell adhesion, the silicone insert was removed, photographed, and then incubated with SRCR for 24 h. Cell images were captured using Nikon ECLIPSE Ti and NIS-Element AR (Version 5.02.01) and analyzed using ImageJ (1.53a) software.

2.13. Cell Migration Assay. An 8.0 μm pore-size transwell chamber (Corning Incorporated, Corning, NY, USA) was used to characterize cell migration. In brief, SCC4 and HSC3 cells (4×10^4 cells) were seeded in the upper chamber. The

lower chamber contained a culture medium with 1% FBS and SRCR at various concentrations. After 24 h, each transwell chamber was fixed using 3.7% formaldehyde for 15 min and stained with 0.05% crystal violet for 30 min. Nonmigrating OSCC cells were removed using cotton swabs. The number of cells was captured using Nikon ECLIPSE Ti and NIS-Element AR (Version 5.02.01) and quantified using ImageJ (1.53a) software.

2.14. Total RNA Extraction and Real-Time PCR Assay. The total RNA of OSCC cells was isolated and reverse transcribed to complementary DNA (cDNA) using an RT-PCR kit (PCR Biosystems Ltd., London, UK). Quantitative PCR was determined using the CFX Connect Real-Time System (Bio-Rad Laboratories Inc., CA, USA) in accordance with the manufacturer's instructions. The raw data and quantification results were normalized to a reference gene, i.e., GAPDH, and mRNA expression levels were calculated as $\text{RQ} = 2^{-\Delta\Delta\text{Ct}}$. All mRNA expression was obtained from four repeated experiments.

2.15. Statistics. Results are presented as mean \pm standard deviation (SD). Statistical analysis between two groups was performed by using Student's *t*-test. Statistical analysis involving more than two groups was performed using one-way analysis of variance (ANOVA) with Fisher's least significant difference (LSD) tests. In all cases, $p < 0.05$ was considered statistically significant.

3. Results

3.1. SRCR Induced Cell Death via Cell Apoptosis in Human OSCC Cells. A CCK-8 assay was first used to characterize the viability of OSCC cells treated with SR, CR, or SRCR at various concentrations (0–480 $\mu\text{g}/\text{mL}$) for 48 h. We found that the IC_{50} values of SRCR in SCC4 and HSC3 cells were 110 $\mu\text{g}/\text{mL}$ and 91 $\mu\text{g}/\text{mL}$, respectively, which were significantly better than treatment with SR or CR alone in both cell lines. Note that SRCR did not affect normal primary gingival fibroblasts (HGF-1) (Figures 1(a)–1(c)). Cisplatin was used as a positive control in cell viability experiments, in which the IC_{50} values for HSC-3 and SCC4 were, respectively, 10 μM and 13 μM (data not shown). Upon SRCR treatment, changes in cell morphology were evaluated in SCC4 and HSC3 cells using DAPI staining. Treatment with different concentrations of SRCR for 48 h induced morphological changes in both cell lines with a corresponding significant decrease in cell number and an increase in chromatin condensation (Figure 1(d)). These results suggest that SRCR can inhibit cell growth and promote cancer cell death in various human OSCC cells.

To clarify the mechanism of cell death caused by SRCR in human OSCC, we performed Annexin V and PI staining of SCC4 and HSC3 cells treated with various concentrations of SRCR (0–480 $\mu\text{g}/\text{mL}$) for 48 hours. The results showed that SRCR concentrations at 240 or 480 $\mu\text{g}/\text{mL}$ were sufficient to induce cell apoptosis, resulting in a higher percentage of late apoptotic cells (annexin-V-positive and PI-positive cells)

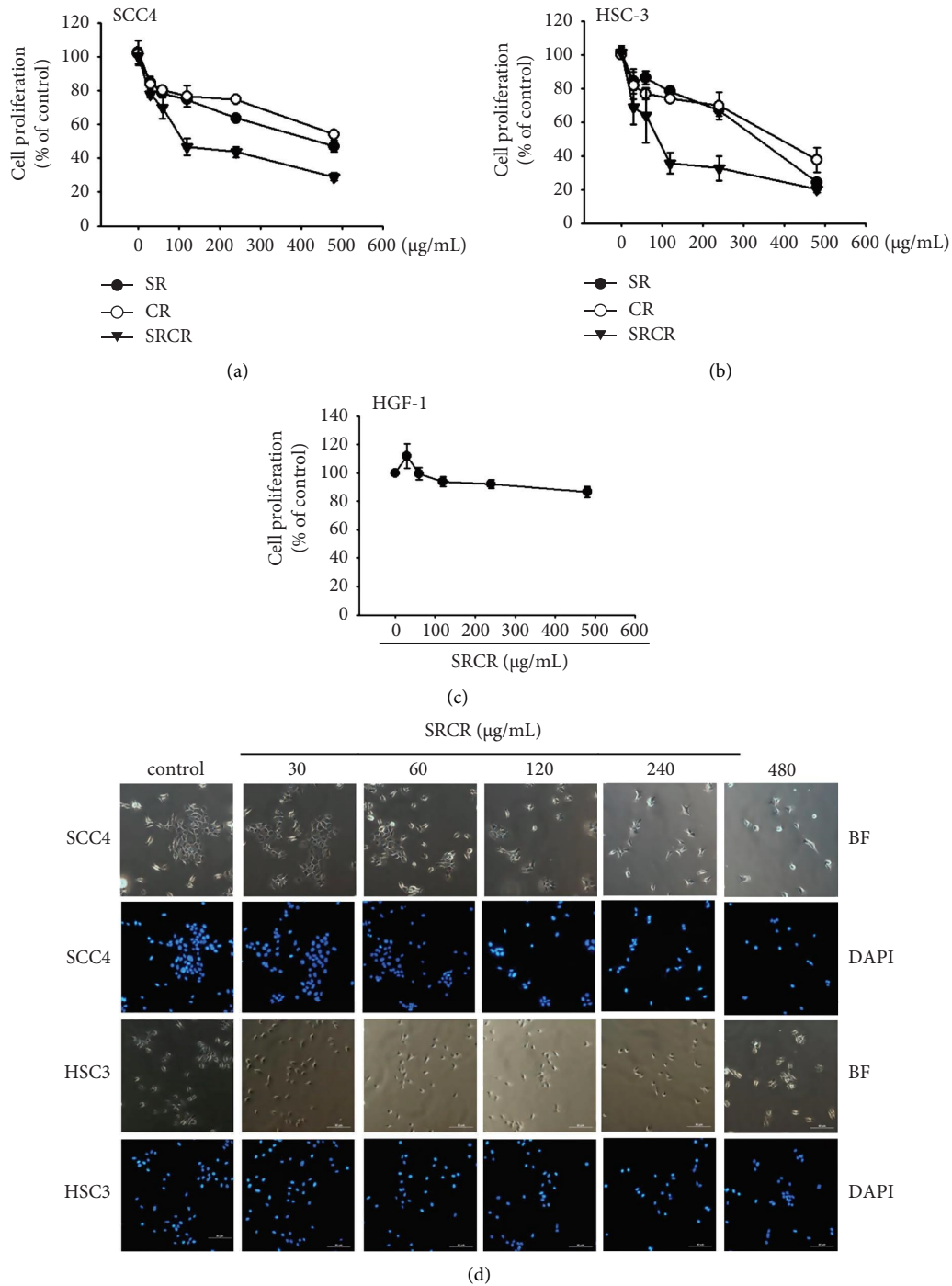


FIGURE 1: SRCR induced cell death in human OSCC cells. (a–c) Cell viability was assessed via a CCK-8 assay following incubation of SCC4, HSC3, and HGF-1 cells with various concentrations of SR, CR, and SRCR for 48 h; (d) after incubating cells with various concentrations of SRCR for 48 h, nucleus morphology was characterized via DAPI staining. Results are expressed as mean ± SD of four independent experiments. * $p < 0.05$ compared to the control group.

and a lower percentage of live cells (annexin-V-negative and PI-negative cells) (Figures 2(a) and 2(b)). A cell cycle assay, which assessed the antiproliferative function of SRCR, performed on SCC4 cells treated with 240 µg/mL or 480 µg/mL SRCR, respectively, revealed a population of hypodiploid

DNA content (sub-G1) at 8.9% and 18.2% (Figure 2(c)). HSC-3 cells treated with SRCR exhibited a similar result: 240 µg/mL (12.5%) and 480 µg/mL (23.7%) (Figure 2(d)). Our findings suggest that the anticancer effects of SRCR are a result of OSCC cell death via the induction of apoptosis.

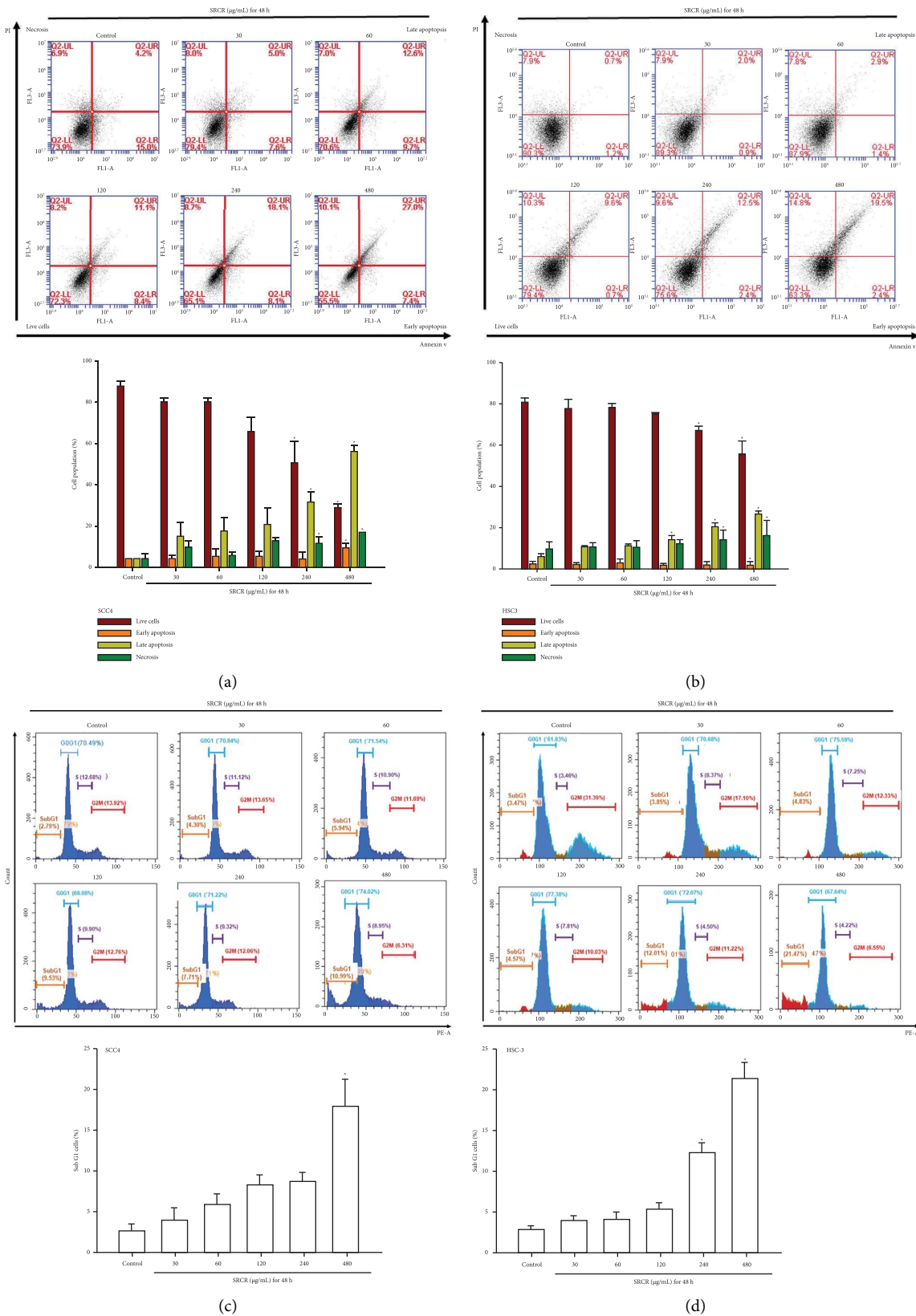


FIGURE 2: SRCR induced cell apoptosis and cell cycle arrest in sub-G1 phase in human OSCC cells. After incubating HSC3 and SCC4 cells with a control solution or SRCR at various concentrations for 48 h, the percentage of apoptotic cells was measured via flow cytometric analysis of (a-b) annexin V and PI double labeling; (c-d) flow cytometry was used to determine the cell cycle distribution of HSC3 and SCC4 cells treated with SRCR at various concentrations (30, 60, 120, 240, and 480 µg/mL) for 48 h. Results are expressed as mean ± SD. * $p < 0.05$ compared to the control group.

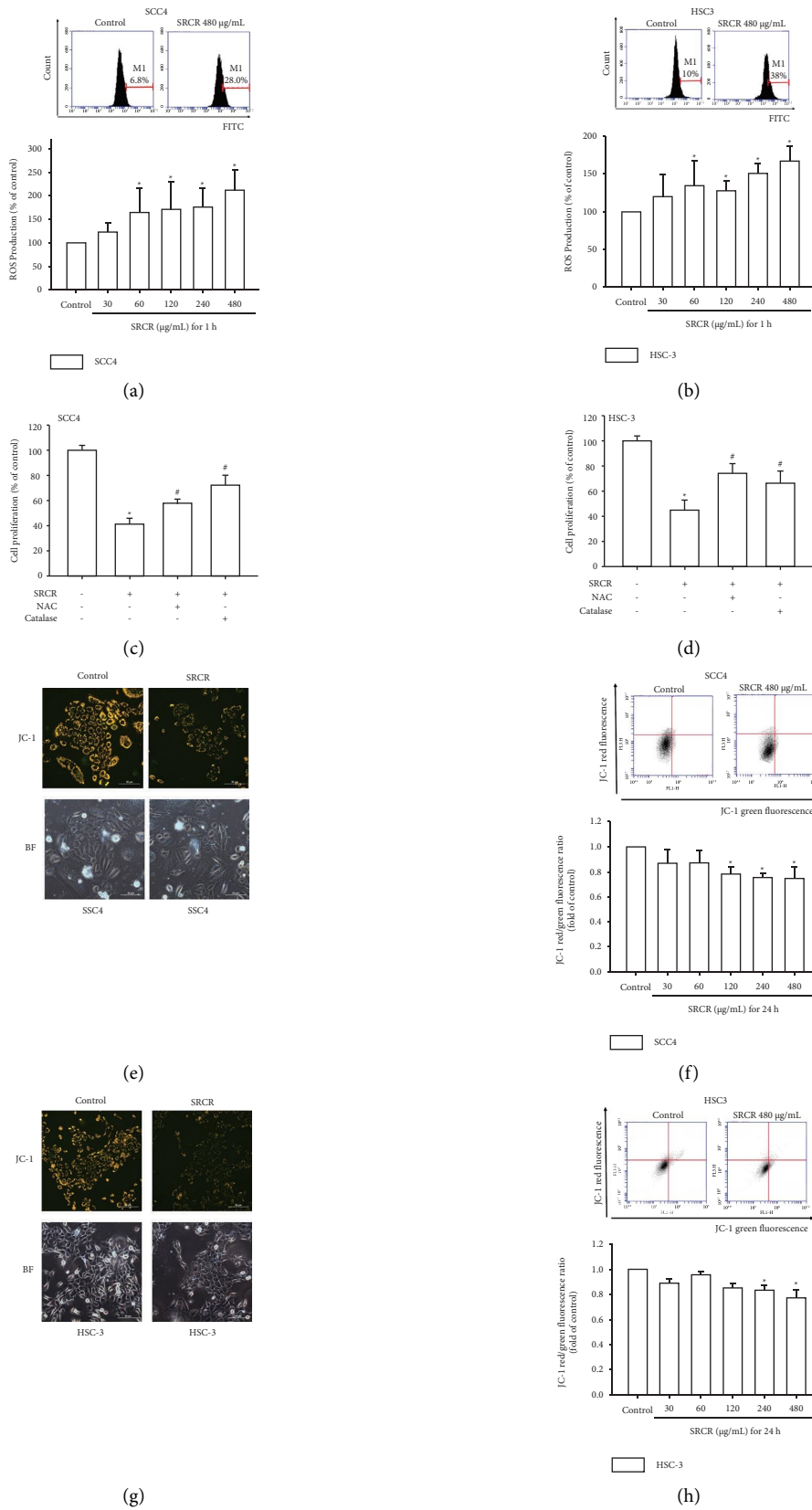


FIGURE 3: Continued.

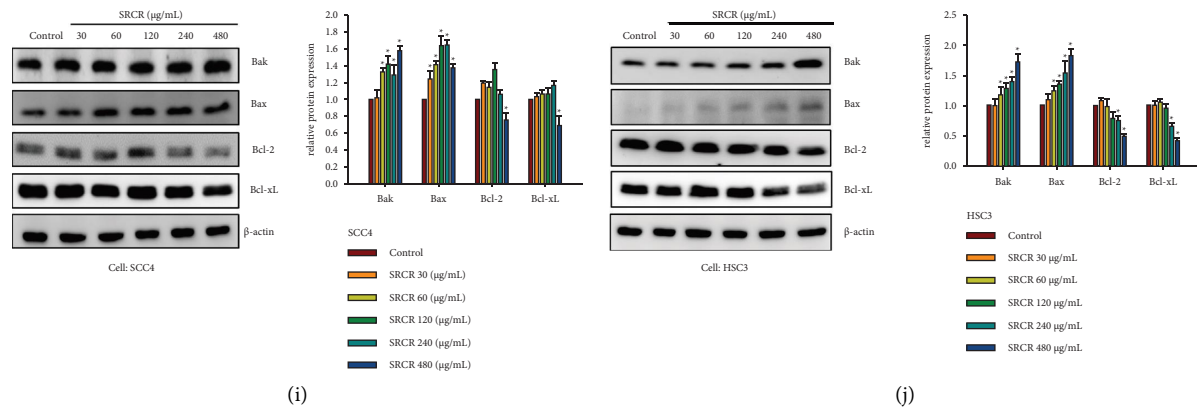


FIGURE 3: SRCR induced ROS production and mitochondrial dysfunction in human OSCC cells. (a–b) After incubating SCC4 and HSC3 cells with various concentrations of SRCR for 1 h, ROS generation was assessed via CM- H_2 DCFDA staining in conjunction with flow cytometric analysis; (c–d) after pretreating cells with catalase (10,000 U/ml) and NAC (5 μ M) for 30 min followed by stimulation using SRCR (240 μ g/mL) for 48 h, cell viability was examined via a CCK-8 assay; (e–h) after incubating SCC4 and HSC3 cells with various concentrations of SRCR for 24 h, MMP was examined via flow cytometry with JC-1 staining; (i–j) after treating cells with different concentrations of SRCR for 24 h, the expression levels of Bcl-2, Bcl-xL, Bak, and Bax were determined using western blot analysis. Results are expressed as mean \pm SD of four independent experiments. * $p < 0.05$ compared to the control group; # $p < 0.05$ compared to the SRCR-treated group.

3.2. SRCR Triggered ROS Production and Mitochondrial Dysfunction in Human OSCC Cells. ROS serves as an antitumor agent and plays a key role in cell apoptosis [14, 15]. To determine whether SRCR-induced apoptosis was a consequence of oxidative stress, intracellular ROS levels were measured using fluorescent ROS probes (H_2 DCFDA). Our data revealed that SRCR treatment for 1 h significantly induced cellular ROS production in a dose-dependent manner (Figures 3(a) and 3(b)). To confirm whether SRCR-mediated ROS generation was correlated with SRCR-mediated cell death, SCC4 and HSC3 cells were pretreated with ROS scavengers (*N*-acetylcysteine (NAC)) and an H_2O_2 scavenging enzyme (catalase) for 30 min prior to the addition of SRCR. The results showed that pretreatment with NAC and catalase indeed mitigated SRCR-induced cell death (Figures 3(c) and 3(d)), suggesting that SRCR-induced cell apoptosis is mediated by a ROS-dependent pathway.

Given that several studies have reported a correlation between the initiation of apoptosis and ROS, which is often associated with mitochondrial damage that leads to alterations in the mitochondrial membrane potential (MMP) [16, 17], we used the fluorescent dye JC-1 to detect MMP in SRCR-treated SCC4 and HSC3 cells. OSCC cells incubated with SRCR exhibited an enhanced intensity of green fluorescence and a decreased intensity of red fluorescence in a concentration-dependent manner, thereby indicating a decrease in MMP (Figures 3(e)–3(h)). As mitochondrial dysfunction is mediated by the Bcl-2 protein family [16], we investigated the expression of proapoptotic and antiapoptotic proteins following SRCR treatment. We found that SRCR-induced proapoptotic multimotif proteins (Bax and Bak) and decreased antiapoptotic proteins (Bcl-2 and Bcl-xL) in a concentration-dependent manner (Figures 3(i) and 3(j)). These results suggest that SRCR-promoted ROS production and mitochondrial dysfunction are involved in apoptosis in OSCC cells.

3.3. SRCR Induced the Proapoptotic Mechanism Regulated by ER Stress in Human OSCC Cells. Oxidative stress accelerates the formation of misfolded proteins and stress responses in the endoplasmic reticulum (ER) [18, 19]. Aberrant calcium homeostasis in the ER from stress also triggers apoptotic cell death [20]. To investigate whether SRCR induces apoptosis through ER stress activation, SCC4 and HSC3 cells were treated with various concentrations of SRCR for 5 h. Our results showed that SRCR treatment significantly increased Ca^{2+} levels in OSCC cells (Figures 4(a) and 4(b)). In addition, an examination of the expression of ER stress-related proteins, such as GRP78, GRP94, calpain I, and calpain II, following treatment with SRCR for 24 h revealed significantly upregulated protein expression of these ER stress-related proteins in both SCC4 and HSC3 cells (Figures 4(c) and 4(d)). Furthermore, pretreating cells with the intracellular calcium chelator BAPTA/AM (10 μ M) abolished SRCR-induced cell death in OSCC cells (Figures 4(e) and 4(f)). These findings suggest that SRCR induces OSCC cell death via aberrant Ca^{2+} release and ER stress.

3.4. SRCR Promoted Apoptotic Signaling via the Caspase Cascade-Dependent Pathway in Human OSCC Cells. To further investigate the mechanisms underlying SRCR-induced apoptosis, we examined the activity and protein expression of two key modulators: caspase 3 and caspase 9. Dose-dependent treatment with SRCR in SCC4 and HSC3 cells significantly increased the activity of caspase 3 and caspase 9 as well as the cleavage of caspase 3 and caspase 9 proteins (Figures 5(a)–5(f)). Furthermore, pretreatment with a caspase-3 inhibitor (z-DEVD-FMK) and caspase-9 inhibitor (z-LEHD-FMK) reduced SRCR-induced apoptosis in OSCC cells (Figures 5(g) and 5(h)). These results indicate that SRCR can induce apoptosis via a caspase-dependent pathway in OSCC cells.

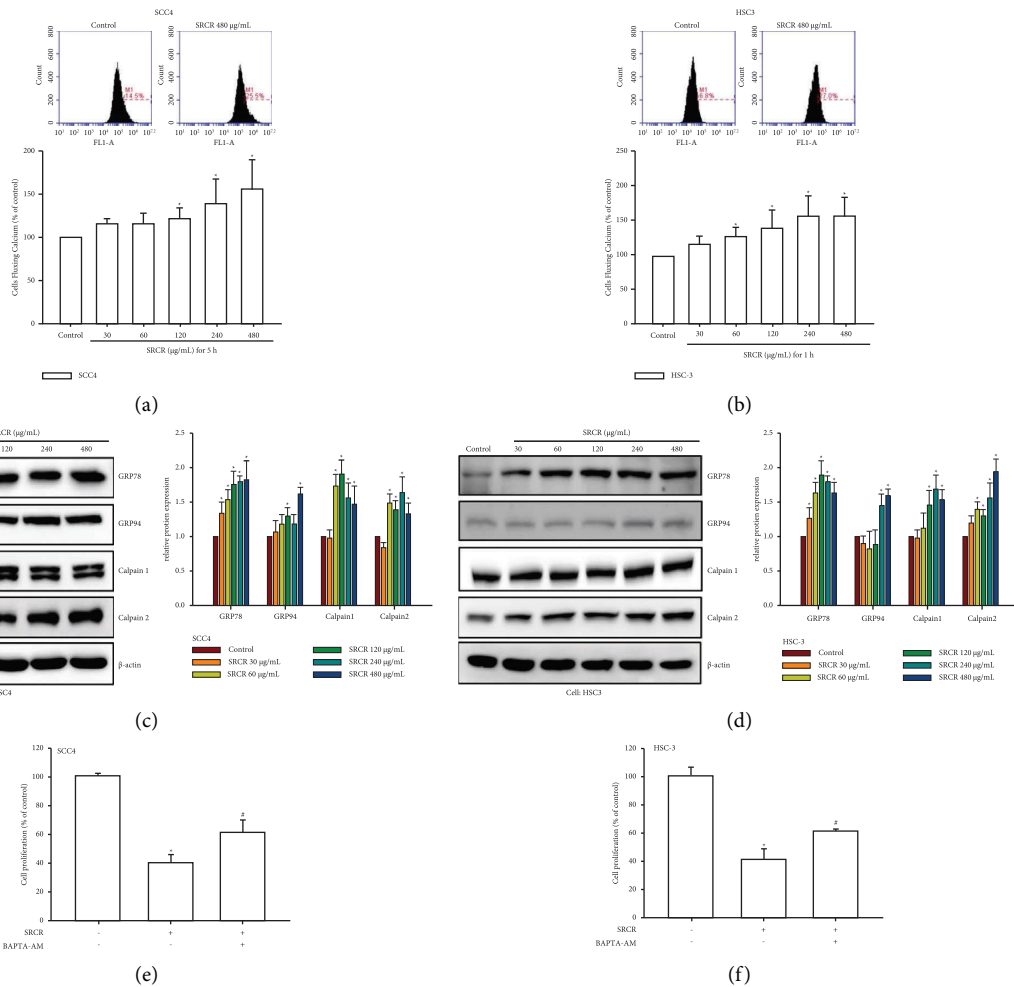


FIGURE 4: SRCR induced Ca²⁺ release and activation of ER stress in human OSCC cells. (a-b) After incubating SCC4 and HSC3 cells with SRCR for 5 h, Ca²⁺ flux was assessed via flow cytometry; (c-d) after incubating cells with SRCR for 24 h, the expression of GRP78, GRP94, calpain I, and calpain II was assessed via western blot analysis; (e-f) after pretreating cells with BAPTA-AM (10 µM) for 30 min and SRCR (240 µg/mL) for 48 h, cell proliferation was analyzed via a CCK-8 assay. Results are expressed as mean ± SD. * *p* < 0.05 compared to the control group; # *p* < 0.05 compared to the SRCR-treated group.

3.5. SRCR Inhibited Cell Migration by Decreasing the Expression of MMP12 and MMP13 in OSCC Cells. As cancer metastasis is a leading cause of death for many OSCC patients [21], we examined the effects of SRCR on the migration of OSCC cells in a wound-healing assay. We found that SRCR at 30–240 µg/mL significantly suppressed the closure rate of the scratch in SCC4 and HSC3 cells when compared to the untreated cells (Figure 6(a)). In addition, cell migration was examined using transwell chambers, in which SCC4 and HSC3 cells were treated with various concentrations of SRCR for 24 h. Our results indicate that SRCR at 60–240 µg/mL significantly, respectively, suppressed the migration of HSC3 and SCC4 cells by 43–79% and 35–73% compared to the control group (Figure 6(b)). Therefore, these results suggest that SRCR reduces cell movement and migration in a dose-dependent manner.

Matrix metalloproteinases (MMPs) have been identified as crucial proteins in tumor cell migration, invasion, and metastasis in OSCC [22, 23]. We found that treatment with

SRCR for 24 h significantly inhibited the expression of MMP-12 and MMP-13 mRNA (Figures 6(c) and 6(d)) and protein expression (Figures 6(e) and 6(f)) in HSC3 and SCC4 cells. Taken together, these results suggest that SRCR inhibits OSCC cell migration by reducing the expression of MMP-12 and MMP-13.

4. Discussion

More than 350,000 new cases of OSCC are diagnosed worldwide each year, leading to approximately 177,000 deaths annually [24]. Conventional treatment strategies for OSCC currently include surgical intervention, chemotherapy, and radiation therapy; however, surgical resection is considered the primary treatment due to the resistance of OSCC to anticancer drugs [25]. Unfortunately, the 5-year overall mortality rate for OSCC patients remains high, exceeding 60% due to the significant risk of metastasis [26].

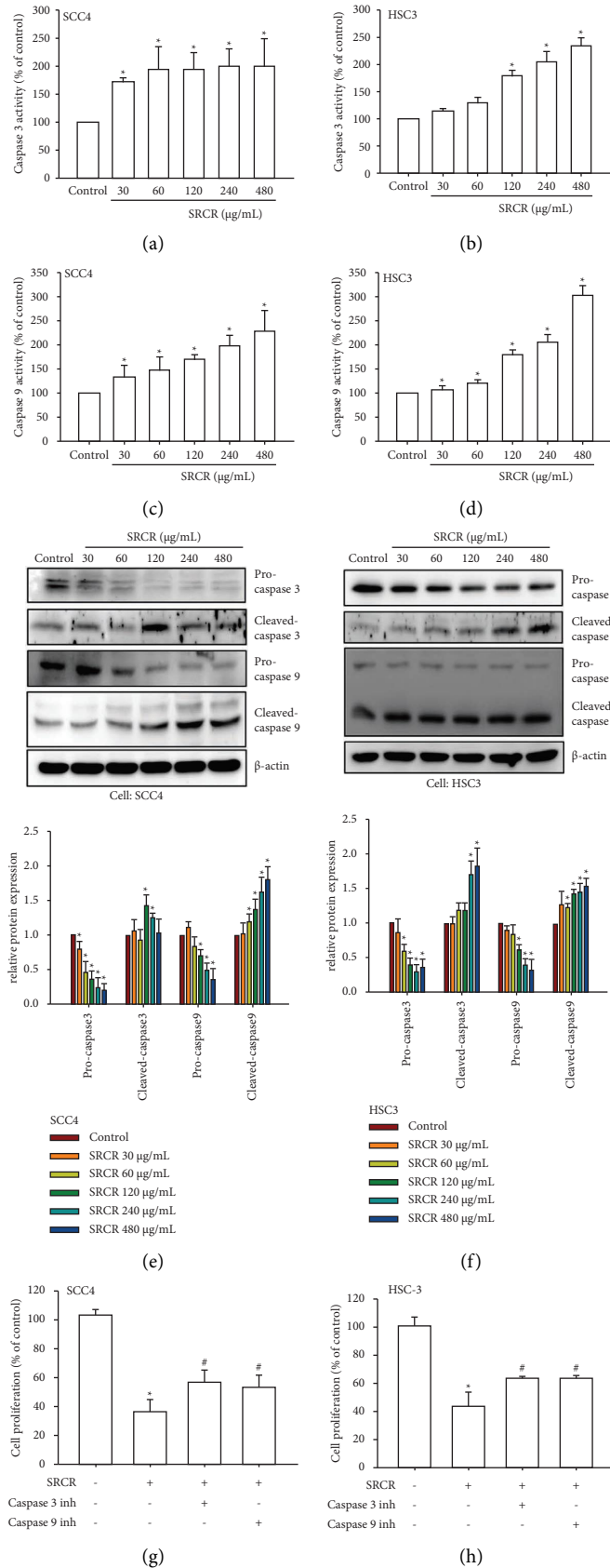


FIGURE 5: SRCR induced activation of caspases in human OSCC cells. (a–d) After incubating SCC4 and HSC3 cells with SRCR for 24 h, caspase-3 and caspase-9 activity was examined using a caspase activity kit; (e–f) after incubating cells with SRCR at various concentrations for 24 h, the expression levels of caspase-3 and caspase-9 proteins were examined via western blot analysis; (g–h) after pretreating cells with a caspase-3 inhibitor (z-DEVD-FMK) or caspase-9 inhibitor (z-LEHD-FMK) for 30 min followed by SRCR stimulation for 48 h, cell proliferation was assessed via a CCK-8 assay. Results are expressed as mean ± SD. * $p < 0.05$ compared to the control group; # $p < 0.05$ compared to the SRCR-treated group.

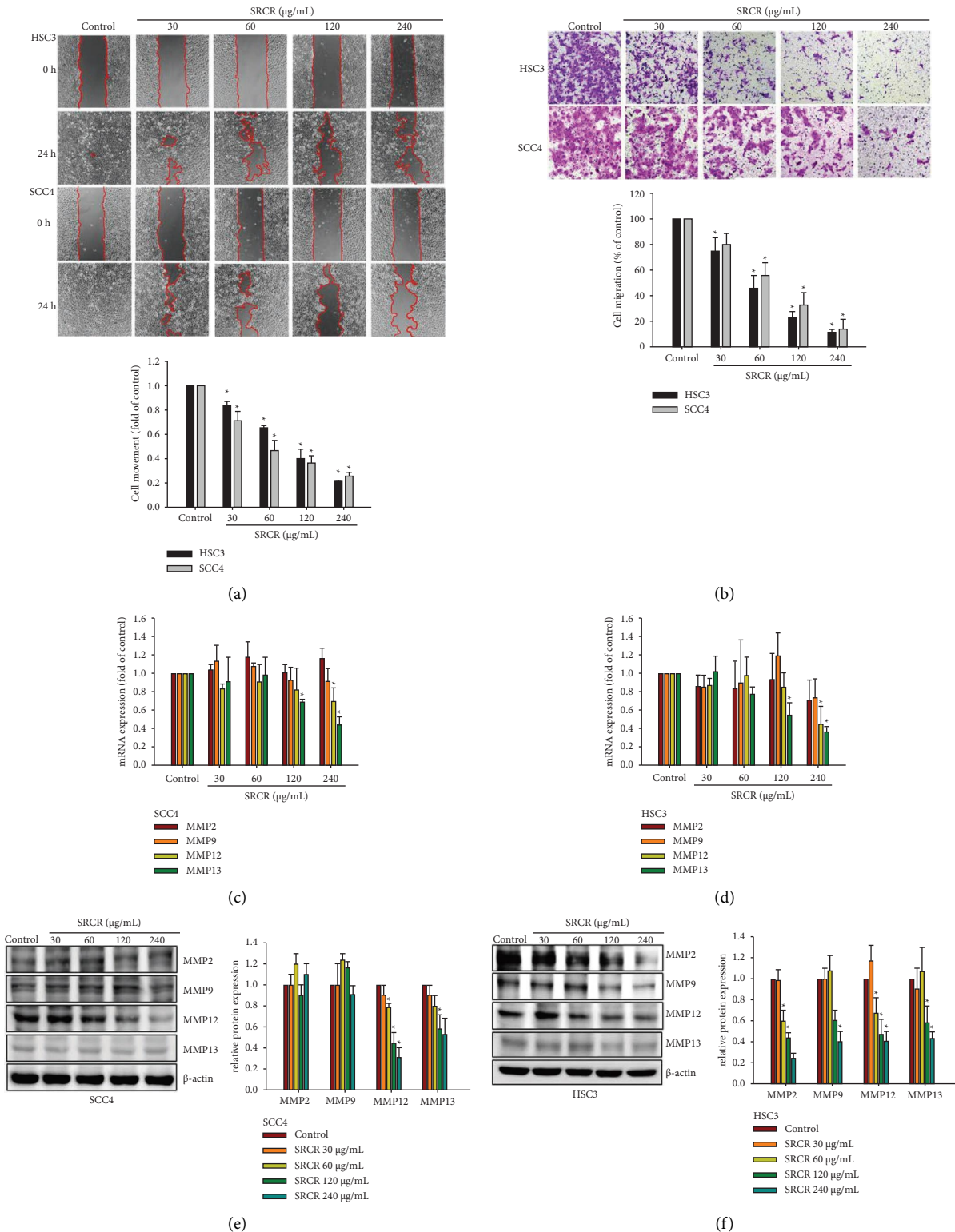


FIGURE 6: SRCR inhibited migration of OSCC cells by modulating expression of MMPs. (a-b) After incubating OSCC cells (HSC3 and SCC4) with a control solution or various concentrations of SRCR for 24 h, cell movement and migration were measured *in vitro* using a wound-healing assay and transwells; (c-f) after incubating OSCC cells (HSC3 and SCC4) with a control solution or various concentrations of SRCR for 24 h, the expression of MMP2, MMP9, MMP12, and MMP13 mRNA and protein was, respectively, examined via qPCR and western blot analysis. Data are expressed as mean \pm SD. * $p < 0.05$ compared to the control group.

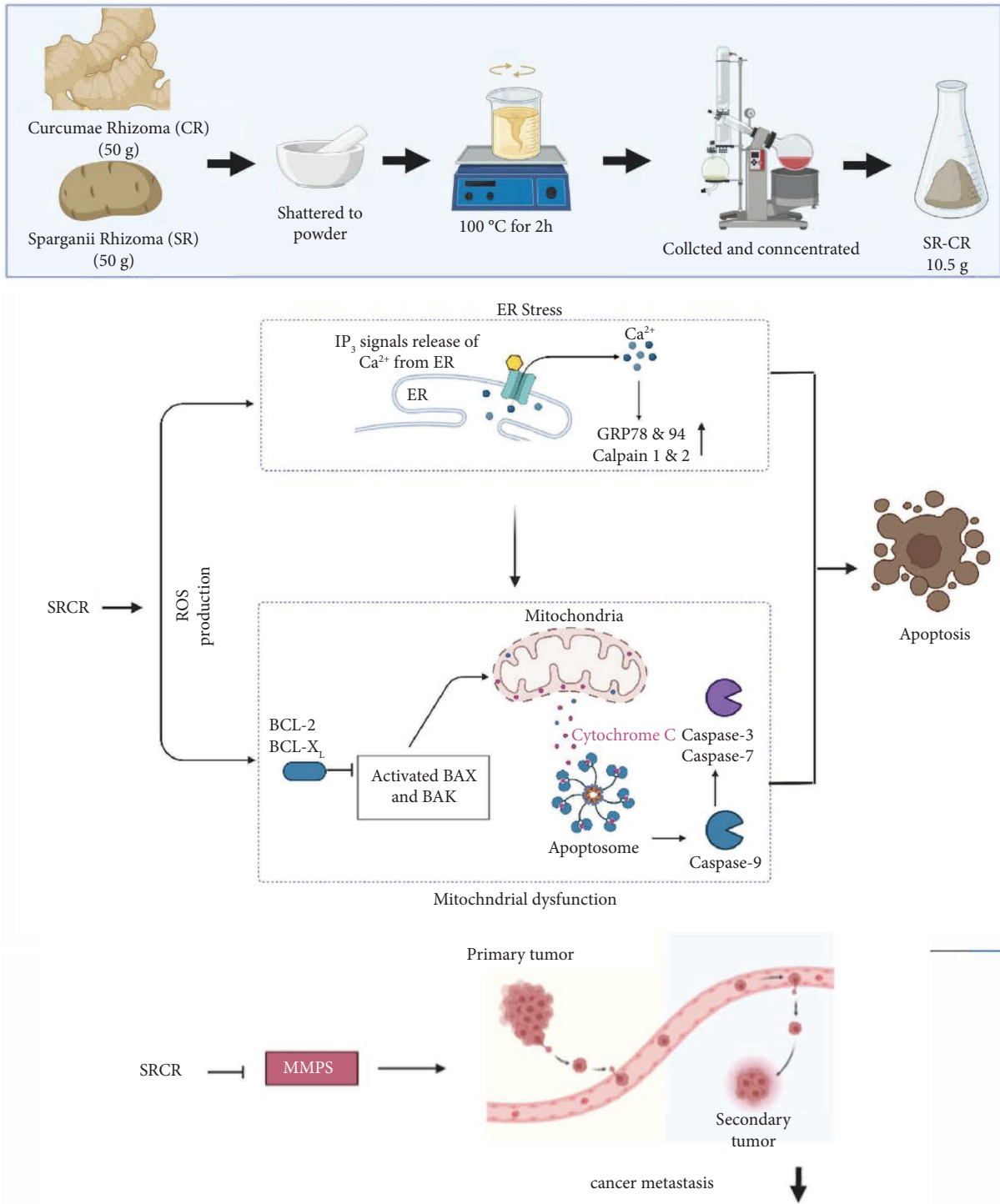


FIGURE 7: Schematic diagram summarize mechanism by which ROS production and ER stress-regulated apoptosis are induced in human OSCC. SR-CR induced apoptotic signaling in OSCC cells by triggering ROS accumulation, ER stress, mitochondrial dysfunction, and caspase activation.

Numerous reports have shown that herb compatibility (herb pairs) is a prevailing matter in traditional Chinese medicine (TCM) [7, 27]. Over the centuries, various herb pairings have been developed and prescribed; however, the underlying mechanisms remain largely unknown. *Sparganii Rhizoma-Curcumae Rhizoma* (SR-CR) is an herbal pair

commonly prescribed in TCM owing to its antithrombosis, antiplatelet, anti-inflammatory, and antiviral activities as well as its ability to promote blood circulation. SR-CR is also used to treat tumors in TCM clinics [9, 28]. Research based on *in vivo* and *in vitro* analysis has demonstrated that the active compounds in extracts of SR and CR exhibit

extraordinary antitumor functions [8, 9, 29]. Specifically, SR has been shown to suppress HeLa cell growth and viability while increasing cell apoptotic signaling [8]. SR also exhibits cytotoxic effects in A549 and MCF-7 cells. The effect of SR on cell cycle is attributed to arrest in the S/G2 phase of cell division [30, 31]. In addition, CR has demonstrated broad-spectrum antitumor functions in several types of cancer, including cell cycle arrest, apoptosis, and the suppression of metastasis [32, 33]. In 2019, Chang et al. provided evidence that the antitumor function of the SRCR decoction segment was superior to that of CR or SR alone against five tumor cell lines (A549, BGC-823, HeLa, HepG2, and MCF-7) [12]. However, the antitumor effects of SRCR in oral cancer remain unclear. This is the first study to report that the antitumor effects of SRCR involve targeting multiple functions in OSCC cells, demonstrating that SRCR-induced cell apoptosis involves ROS generation, ER stress, mitochondrial dysfunction, and finally, caspase activation. As conventional therapies for OSCC are largely ineffective in terms of prognosis, these findings suggest that this combination of two TCMs may provide an alternative cancer treatment that could enhance therapeutic outcomes.

Lymphatic metastasis is a common occurrence in OSCC, resulting in regional metastases in 40% of patients and distant metastasis in 15% of patients [34]. The median survival for those with metastatic OSCC is only three months [35]. The process of metastasis involves cancer cell migration from the primary site followed by the formation of a secondary tumor at a distant site [36]. The involvement of MMPs in tumor disruption, tumor neovascularization, and metastasis indicates their potential as prognostic markers and therapeutic targets [37]. Furthermore, our results showed that SRCR inhibits OSCC cell migration by decreasing the expression of MMP12 and MMP13. This preliminary research revealed the role of SRCR in inhibiting cell migration as well as novel insights into the inhibitory effects of SRCR.

5. Conclusions

This study aimed to address the limitations of conventional therapy for human OSCC. Our results demonstrate that an aqueous extract of SRCR induced cell apoptosis through ROS production, mitochondrial dysfunction, and ER stress signaling. In addition, we found that SRCR inhibited OSCC cell migration by reducing the expression of MMP12 and MMP13 (Figure 7). These findings suggest that SRCR could potentially be an alternative therapeutic agent for the treatment of OSCC.

Abbreviations

OSCC:	Oral squamous cell carcinoma
SRCR:	<i>Sparganii Rhizoma</i> and <i>Curcumae Rhizoma</i>
ROS:	Reactive oxygen species
ER:	Endoplasmic reticulum
GRP:	Glucose-regulated proteins
Bax:	B cell lymphoma-2 associated-x protein

Bak:	B cell lymphoma-2 homologous antagonist/killer
MMP:	Mitochondrial membrane potential
TCM:	Traditional Chinese medicine
H2DCFDA:	2',7'-dichlorodihydrofluorescein diacetate
PI:	Propidium iodide
FITC:	Fluorescein isothiocyanate
ANOVA:	Analysis of variance
SD:	Standard deviation
NAC:	N-acetylcysteine.

Data Availability

The data that support the findings of this study are available from the corresponding author upon reasonable request.

Conflicts of Interest

The authors declare that there are no conflicts of interest.

Authors' Contributions

K. W. Chang, C. Y. Wu, Y. Y. Kung, and J. F. Liu conceived and designed the experiments. T. Y. Renn, T. M. Chang, and C. Y. Wu contributed reagents, materials, and analytical tools. K. W. Chang and J. F. Liu wrote the paper. K. W. Chang, Y. Y. Kung, and J. F. Liu contributed to the final manuscript.

Acknowledgments

This work was supported by grants from the Ministry of Science and Technology in Taiwan (MOST-106-2314-B-038-099-MY3 and MOST111-2321-B-A49-007), Taipei Medical University (TMU108-AE1-B47), and Taipei Veterans General Hospital (V110C-098).

References

- [1] C. Rivera, "Essentials of oral cancer," *International Journal of Clinical and Experimental Pathology*, vol. 8, no. 9, pp. 11884–11894, 2015.
- [2] A. K. D'Cruz, R. Vaish, and H. Dhar, "Oral cancers: current status," *Oral Oncology*, vol. 87, pp. 64–69, 2018.
- [3] C. S. Farah, "Molecular landscape of head and neck cancer and implications for therapy," *Annals of Translational Medicine*, vol. 9, no. 10, p. 915, 2021.
- [4] D. V. Messadi, "Diagnostic aids for detection of oral precancerous conditions," *International Journal of Oral Science*, vol. 5, no. 2, pp. 59–65, 2013.
- [5] T. K. Ong, C. Murphy, A. B. Smith, A. N. Kanatas, and D. A. Mitchell, "Survival after surgery for oral cancer: a 30-year experience," *British Journal of Oral and Maxillofacial Surgery*, vol. 55, no. 9, pp. 911–916, 2017.
- [6] A. K. Sah, A. Vyas, P. K. Suresh, and B. Gidwani, "Application of nanocarrier-based drug delivery system in treatment of oral cancer," *Artificial Cells, Nanomedicine, and Biotechnology*, vol. 46, no. 4, pp. 650–657, 2018.
- [7] S. Wang, Y. Hu, W. Tan et al., "Compatibility art of traditional Chinese medicine: from the perspective of herb pairs," *Journal of Ethnopharmacology*, vol. 143, no. 2, pp. 412–423, 2012.

- [8] G. L. Xu, D. Geng, M. Xie et al., "Chemical composition, antioxidative and anticancer activities of the essential oil: curcumae rhizoma-sparganii rhizoma, a traditional herb pair," *Molecules*, vol. 20, no. 9, pp. 15781–15796, 2015.
- [9] Y. L. Chang, G. L. Xu, X. P. Wang et al., "Anti-tumor activity and linear-diarylheptanoids of herbal couple Curcumae Rhizoma-Sparganii Rhizoma and the single herbs," *Journal of Ethnopharmacology*, vol. 250, Article ID 112465, 2020.
- [10] Y. Feng, Y. Zhao, Y. Li et al., "Inhibition of fibroblast activation in uterine leiomyoma by components of rhizoma curcumae and rhizoma sparganii," *Frontiers in Public Health*, vol. 9, Article ID 650022, 2021.
- [11] S. Dai, G. Zhang, F. Zhao, and Q. Shu, "Study on the molecular mechanism of the herbal couple sparganii rhizoma-curcumae rhizoma in the treatment of lung cancer based on network pharmacology," *Evidence-based Complementary and Alternative Medicine*, vol. 2021, Article ID 6664489, 17 pages, 2021.
- [12] Y. Yin, L. Feng, L. Wang, and L. Ding, "The role of curcumae rhizoma-sparganii rhizoma medicated serum in epithelial-mesenchymal transition in the triple negative breast cancer: pharmacological role of CR-SR in the TBNC," *Biomedicine & Pharmacotherapy*, vol. 99, pp. 340–345, 2018.
- [13] J. F. Liu, C. H. Hou, F. L. Lin, Y. T. Tsao, and S. M. Hou, "Nimbolide induces ROS-regulated apoptosis and inhibits cell migration in osteosarcoma," *International Journal of Molecular Sciences*, vol. 16, no. 10, pp. 23405–23424, 2015.
- [14] S. Yasuda, S. Yogosawa, Y. Izutani, Y. Nakamura, H. Watanabe, and T. Sakai, "Cucurbitacin B induces G2 arrest and apoptosis via a reactive oxygen species-dependent mechanism in human colon adenocarcinoma SW480 cells," *Molecular Nutrition & Food Research*, vol. 54, no. 4, pp. 559–565, 2010.
- [15] C. Y. Chuang, H. C. Liu, L. C. Wu, C. Y. Chen, J. T. Chang, and S. L. Hsu, "Gallic acid induces apoptosis of lung fibroblasts via a reactive oxygen species-dependent ataxia telangiectasia mutated-p53 activation pathway," *Journal of Agricultural and Food Chemistry*, vol. 58, no. 5, pp. 2943–2951, 2010.
- [16] K. Ksiezakowska-Lakoma, M. Zyla, and J. R. Wilczyński, "Mitochondrial dysfunction in cancer," *Menopause Review*, vol. 2, no. 2, pp. 136–144, 2014.
- [17] A. Rasul, J. Di, F. M. Millimouno et al., "Reactive oxygen species mediate isoalantolactone-induced apoptosis in human prostate cancer cells," *Molecules*, vol. 18, no. 8, pp. 9382–9396, 2013.
- [18] P. Zou, J. Zhang, Y. Xia et al., "ROS generation mediates the anti-cancer effects of WZ35 via activating JNK and ER stress apoptotic pathways in gastric cancer," *Oncotarget*, vol. 6, no. 8, pp. 5860–5876, 2015.
- [19] P. Walter and D. Ron, "The unfolded protein response: from stress pathway to homeostatic regulation," *Science*, vol. 334, no. 6059, pp. 1081–1086, 2011.
- [20] S. J. Park, Y. Kim, S. M. Yang et al., "Discovery of endoplasmic reticulum calcium stabilizers to rescue ER-stressed podocytes in nephrotic syndrome," *Proceedings of the National Academy of Sciences of the U S A*, vol. 116, no. 28, pp. 14154–14163, 2019.
- [21] C. C. Chao, C. W. Lee, T. M. Chang, P. C. Chen, and J. F. Liu, "CXCL1/CXCR2 paracrine Axis contributes to lung metastasis in osteosarcoma," *Cancers*, vol. 12, no. 2, p. 459, 2020.
- [22] P. Yin, Y. Su, S. Chen et al., "MMP-9 knockdown inhibits oral squamous cell carcinoma lymph node metastasis in the nude mouse tongue-xenografted model through the RhoC/src pathway," *Analytical Cellular Pathology*, vol. 2021, Article ID 6683391, 16 pages, 2021.
- [23] C. Y. Chan, T. Y. Lin, J. J. Sheu, W. C. Wu, and C. Y. Huang, "Matrix metalloproteinase-13 is a target gene of high-mobility group box-containing protein 1 in modulating oral cancer cell invasion," *Journal of Cellular Physiology*, vol. 234, no. 4, pp. 4375–4384, 2019.
- [24] S. H. Chen, S. Y. Hsiao, K. Y. Chang, and J. Y. Chang, "New insights into oral squamous cell carcinoma: from clinical aspects to molecular tumorigenesis," *International Journal of Molecular Sciences*, vol. 22, no. 5, p. 2252, 2021.
- [25] L. E. Moses, J. M. Rotsides, F. O. Balogun, M. S. Persky, F. M. Muggia, and M. J. Persky, "Oral squamous cell carcinoma as a complication of treatment for recurrent high-grade serous cancer," *The Laryngoscope*, vol. 130, no. 11, pp. 2607–2610, 2020.
- [26] S. R. Quinlan-Davidson, A. S. R. Mohamed, J. N. Myers et al., "Outcomes of oral cavity cancer patients treated with surgery followed by postoperative intensity modulated radiation therapy," *Oral Oncology*, vol. 72, pp. 90–97, 2017.
- [27] W. X. Li, H. Zhang, J. F. Tang et al., "[Clinical application characteristics of Danggui-Chuanxiong herb pair in Chinese medicines on basis of real-world]," *Zhongguo Zhongyao Zazhi*, vol. 41, no. 7, pp. 1338–1341, 2016.
- [28] X. Y. Liu, Y. L. Chang, X. H. Wang et al., "An integrated approach to uncover anti-tumor active materials of Curcumae Rhizoma-Sparganii Rhizoma based on spectrum-effect relationship, molecular docking, and ADME evaluation," *Journal of Ethnopharmacology*, vol. 280, Article ID 114439, 2021.
- [29] J. L. Gao, T. C. He, Y. B. Li, and Y. T. Wang, "A traditional Chinese medicine formulation consisting of Rhizoma Corydalis and Rhizoma Curcumae exerts synergistic anti-tumor activity," *Oncology Reports*, vol. 22, no. 5, pp. 1077–1083, 2009.
- [30] J. Jia, X. Li, X. Ren et al., "Sparganii Rhizoma: a review of traditional clinical application, processing, phytochemistry, pharmacology, and toxicity," *Journal of Ethnopharmacology*, vol. 268, Article ID 113571, 2021.
- [31] J. W. Zhang and Y. H. Wei, "Retracted article: anti-cancer effects of grailsine-al-glycoside isolated from Rhizoma Sparganii," *BMC Complementary and Alternative Medicine*, vol. 14, no. 1, p. 82, 2014.
- [32] Y. Chen, Z. Zhu, J. Chen et al., "Terpenoids from Curcumae Rhizoma: their anticancer effects and clinical uses on combination and versus drug therapies," *Biomedicine & Pharmacotherapy*, vol. 138, Article ID 111350, 2021.
- [33] Y. H. Bi, L. H. Zhang, S. J. Chen, and Q. Z. Ling, "Antitumor mechanisms of curcumae rhizoma based on network pharmacology," *Evidence-based Complementary and Alternative Medicine*, vol. 2018, Article ID 4509892, 9 pages, 2018.
- [34] J. J. Caudell, M. L. Gillison, E. Maghami et al., "NCCN Guidelines® insights: head and neck cancers, version 1.2022: featured updates to the NCCN guidelines," *Journal of the National Comprehensive Cancer Network*, vol. 20, no. 3, pp. 224–234, 2022.
- [35] A. Hosni, S. H. Huang, W. Xu et al., "Distant metastases following postoperative intensity-modulated radiotherapy for oral cavity squamous cell carcinoma," *JAMA Otolaryngol Head Neck Surg*, vol. 143, no. 4, pp. 368–375, 2017.
- [36] M. J. Allegranza and J. R. Conejo-Garcia, "Targeted therapy and immunosuppression in the tumor microenvironment," *Trends in Cancer*, vol. 3, no. 1, pp. 19–27, 2017.
- [37] B. Shrestha, D. Bajracharya, A. A. Byatnal, A. Kamath, and R. Radhakrishnan, "May high MMP-2 and TIMP-2 expressions increase or decrease the aggressivity of oral cancer?" *Pathology and Oncology Research*, vol. 23, no. 1, pp. 197–206, 2017.